insoluble in water, acetone, chloroform, and diethyl ether, whereas slightly soluble in dilute sulfuric acid; soluble in hot alcohol and dilute alkali solutions [12].

Improvement of the physicochemical properties is very important for the improvement of solubility, dissolution, absorption, and bioavailability of the pharmaceutical and nutraceutical compounds [13]. In this regard, The Trivedi Effect®-Biofield Energy Healing Treatment has a significant effect on various properties such as particle size, surface area, bioavailability and isotopic abundance ratios of pharmaceutical and nutraceutical compounds [14-18]. The Trivedi Effect® is a natural and only scientifically proven phenomenon in which a person can harness this inherently intelligent energy and transmit it anywhere on the planet through the possible mediation of neutrinos [19]. "Biofield Energy" the electromagnetic energy field which exists surrounding the living beings, which can transmit the electromagnetic energy in the form of bio-photons, generated by the continuous movement of the electrically charged particles (ions, cells, etc.) inside the body. Biofield Energy Healing specialists can harness the energy from the environment or the "Universal Energy Field" and can transmit into any living and non-living object(s), this process is called Biofield Energy Healing Treatment [20-22]. Biofield based Energy Therapies have been reported with significant outcomes against various disease [23]. The National Center of Complementary and Integrative Health (NCCIH) has recognized and accepted Biofield Energy Healing as a Complementary and Alternative Medicine (CAM) health care approach in addition to other therapies, medicines, and practices such as yoga, Qi Gong, Tai Chi, hypnotherapy, Reiki, etc. [24,25]. These therapies have been accepted by most of the U.S.A. population with several advantages [25]. The Trivedi Effect®-Consciousness Energy Healing Treatment has been reported with the significant revolution in the metals, chemicals, ceramics and polymers, crops, microbes, biotechnology, skin health, bone health, cancer cell line, etc. [24-38]. The Trivedi Effect®-Biofield Energy Healing Treatment could be an economical approach for the practical problems associated with 6-mercaptopurine for the physicochemical properties for designing better pharmaceutical formulations. The stable isotope ratio analysis has various applications in different scientific fields for understanding the isotope effects resulting from the variation of the isotopic composition of the molecule [39,40]. Isotope ratio analysis can be performed by using the conventional mass spectrometry (MS) techniques such as gas chromatography-mass spectrometry (GC-MS) and liquid chromatography-mass spectrometry (LC-MS) in low micromolar concentration with sufficient precision [39,41]. Therefore, LC-MS and GC-MS were used in this study to characterize the structural properties and evaluate the isotopic abundance ratio analysis of P_{M+1}/P_M ($^2H/^1H$ or $^{13}C/^{12}C$ or $^{15}N/^{14}N$ or $^{33}S/^{32}S$) and P_{M+2}/P_M ($^{33}S/^{32}S$) in The Trivedi Effect® - Consciousness Energy Healing treated 6-mercaptopurine compared to the control sample.

MATERIALS AND METHODS

Chemicals and reagents

6-mercaptopurine was purchased from Tokyo Chemical Industry Co., Ltd., Japan. Other chemicals used during the experiments were of analytical grade available in India.

Consciousness Energy Healing Treatment Strategies

The 6-mercaptopurine powder was the test sample divided into two parts. One part of the 6-mercaptopurine powder sample was considered as a control sample (no Biofield Energy Treatment was provided). However, the other part of 6-mercaptopurine was treated with The Trivedi Effect®-Consciousness Energy Healing Treatment remotely under standard laboratory conditions for 3 minutes and known as The Trivedi Effect® Treated or Biofield Energy Treated 6-mercaptopurine sample. The Biofield Energy Treatment was provided through the healer's unique energy transmission process by the renowned Biofield Energy Healer, Alice Branton, USA, to the test sample. Further, the control sample was treated with a "sham" healer for comparison purposes. The sham healer did not have any knowledge about the Biofield Energy Treatment. After that, the Biofield Energy Treated and untreated 6-mercaptopurine samples were kept in sealed conditions and characterized using LC-MS and GC-MS, analytical techniques.

CHARACTERIZATION

Liquid chromatography-mass spectrometry (LC-MS) analysis and Calculation of Isotopic Abundance Ratio

The LC-MS analysis of the control and Biofield Energy Treated 6-mercaptopurine was carried out with the help of LC-MS Thermo Fisher Scientific, the USA equipped with an ion trap detector connected with a triple-stage quadrupole mass spectrometer. The column used here was a reversed-phase Thermo Scientific Synchronis C18 (Length-250 mm X ID 4.6 mm X 5 micron), maintained at 25˚C. The diluent used for the sample preparation was acetonitrile and water. 10 µL of the 6-mercaptopurine solution was injected, and the analyte was eluted using 0.1% formic acid in water (mobile phase A; 10%) and acetonitrile (mobile phase B; 95%) pumped at a constant flow rate of 0.5 mL/min. Chromatographic separation was achieved using gradient condition and the total run time was 10 min. Peaks were monitored at 300 nm using the Photo Diode Array (PDA) detector. The mass spectrometric analysis was performed under a +ve ESI mode. The total ion chromatogram, peak area% and mass spectrum of the individual peak which was appeared in LC along with the full scan (*m/z* 50-300) were recorded. The total ion chromatogram and mass spectrum of the individual peak (appeared in LC-MS) were recorded.

The natural abundance of each isotope (C, O, H, N, and S)

can be predicted from the comparison of the height of the isotope peak with respect to the base peak. The values of the natural isotopic abundance of the common elements are obtained from the literature [40,41-44]. The LC-MS based isotopic abundance ratios (P_{M+1}/P_M) for the control and Biofield Energy Treated 6-mercaptopurine was calculated.

Percentage (%) change in isotopic abundance ratio = $[(IAR_{Treated} - IAR_{Control})/ IAR_{Control}) \times 100]$

where $IAR_{Treated}$ = isotopic abundance ratio in the treated sample and $IAR_{Control}$ = isotopic abundance ratio in the control sample.

Gas chromatography-mass spectrometry (GC-MS) analysis

GC-MS of the control and Biofield Energy Treated sample of 6-mercaptopurine were analyzed with the help of Perkin Elmer Gas chromatograph equipped with a PE-5MS (30 M x 250 microns x 0.250 microns) capillary column and coupled to a single quadrupole mass detector was operated with electron impact (EI) ionization in positive mode. The oven temperature was programmed from 180°C (14 min hold) to 290°C (14 min hold) @ 10°C/min (total run time 30 min). The sample was prepared taking 80 mg of the 6-mercaptopurine is in 4 ml acetonitrile and water (1:1) as a diluent. Mass spectra were scanned from *m/z* 20 to 400. The identification of analyte was done by GC retention times and by a comparison of the mass spectra of samples.

The GC-MS based isotopic abundance ratios (P_{M+1}/P_M and P_{M+2}/P_M) for the control and Biofield Energy Treated 6-mercaptopurine was calculated.

Percentage (%) change in isotopic abundance ratio = $[(IAR_{Treated} - IAR_{Control})/ IAR_{Control}) \times 100]$

Where $IAR_{Treated}$ = isotopic abundance ratio in the treated sample and $IAR_{Control}$ = isotopic abundance ratio in the control sample.

RESULTS AND DISCUSSION

Liquid chromatography-mass spectrometry (LC-MS)

The LC-MS chromatograms and mass spectra of both the samples of 6-mercaptopurine are shown in **Figures 1 and 2**, respectively. The chromatograms of 6-mercaptopurine showed the single major chromatographic peak at the retention time (R_t) of 2.24 minutes in the case of both the samples **(Figure 1)**. These results indicated that the polarity of both the control and Biofield Energy Treated 6-mercaptopurine was the same. As per the literature 6-mercaptopurine was detected with the molecular mass peak $[M]^+$ at *m/z* 152 MS spectrum in positive ion mode [12]. The mass spectra of both the samples of 6-mercaptopurine **(Figure 2)** exhibited the mass of the protonated molecular ion peak at *m/z* 153 $[M+H]^+$ (calculated for $C_5H_5N_4S^+$, 153.18) in the control sample and Biofield Energy Treated sample **(Figure 3)**.

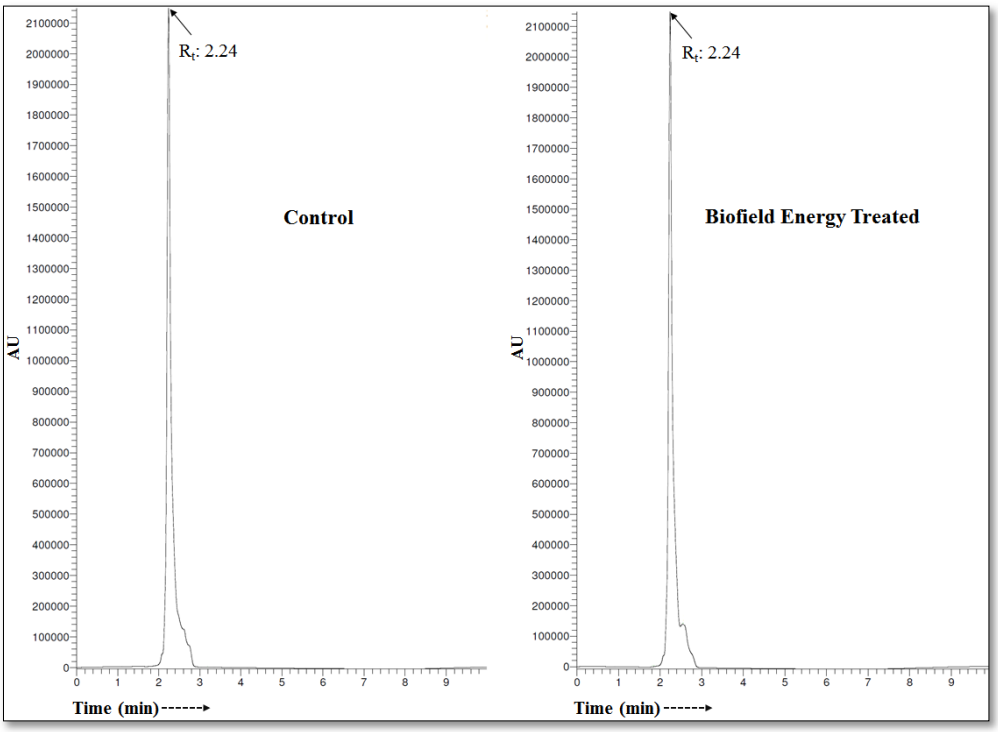

Figure 1. Liquid chromatograms of the control and Biofield Energy Treated 6-mercaptopurine.

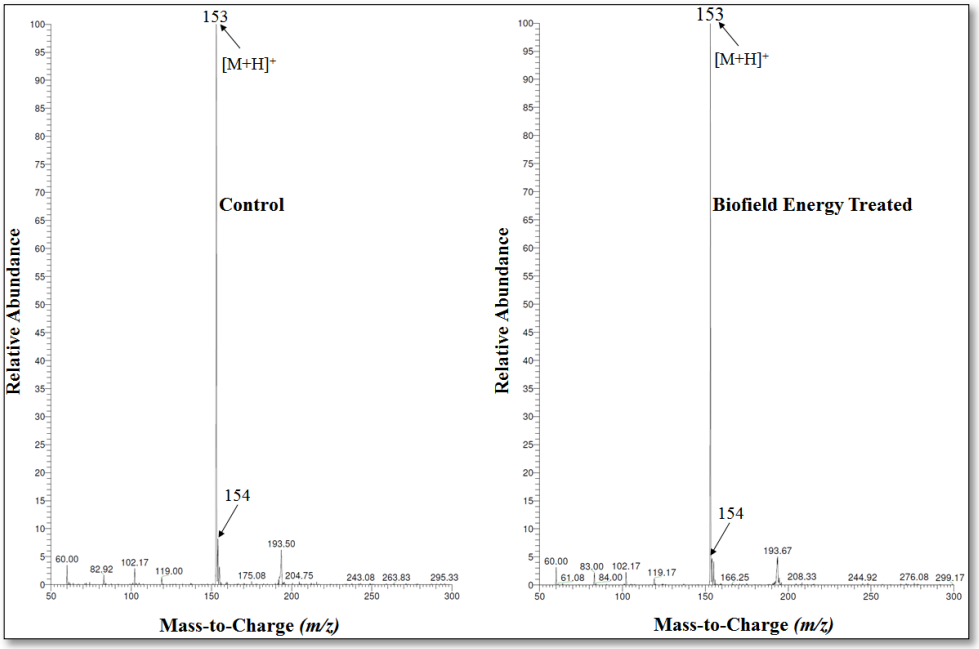

Figure 2. Mass spectra of the control and Biofield Energy Treated 6-mercaptopurine at R_t 2.24 minutes.

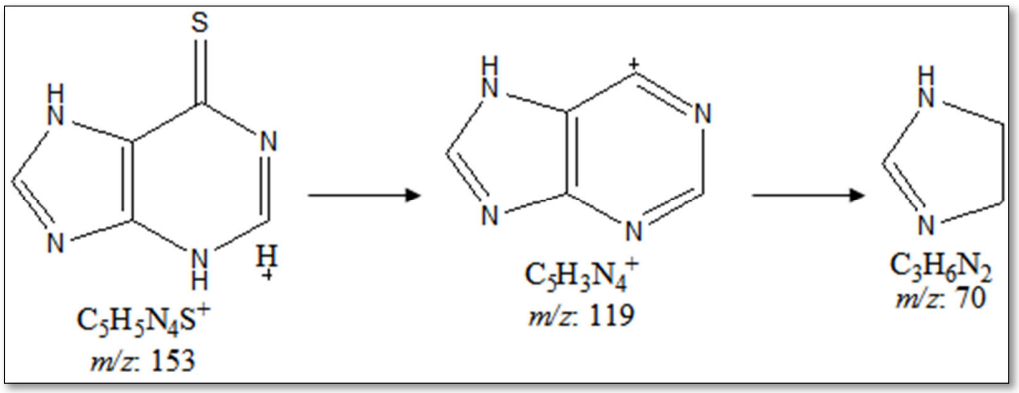

Figure 3. Proposed fragmentation pattern of 6-mercaptopurine.

The LC-MS spectra of both the control and Biofield Energy Treated 6-mercaptopurine showed the mass of the molecular ion peak $[M+H]^+$ at *m/z* 153 $[M+H]^+$ (calculated for $C_5H_5N_4S^+$, 153.18) with the relative intensity of 100%. The theoretical calculation of P_{M+1} for 6-mercaptopurine was presented below:

P (^{13}C) = [(5 x 1.1%) x 100% (the actual size of the M^+ peak)]/100% = 5.5%

P (^{2}H) = [(5 x 0.015%) x 100%] / 100%= 0.075%

P (^{15}N) = [(4 x 0.4%) x 100%] / 100% = 1.6%

P (^{33}S) = [(1 x 0.08%) x 100%] / 100% = 0.08%

$P_{M+1,}$ i.e., ^{13}C, ^{2}H, ^{15}N, and ^{33}S contributions from $(C_5H_5N_4S)^+$ to *m/z* 154= 7.26%

The calculated isotope abundance (7.26%) was close to the experimental value of 8.19% **(Table 1)**. From the above calculation, it has been found that ^{13}C and ^{15}N have a major contribution to *m/z* 154.

The LC-MS based isotopic abundance ratio analysis P_M and P_{M+1} for 6-mercaptopurine near *m/z* 153 and 154, respectively of the control and Biofield Energy Treated samples, which were obtained from the observed relative peak intensities of $[M^+]$ and $[(M+1)^+]$ peaks, respectively in the ESI-MS spectra **(Table 1)**. The percentage change of the isotopic abundance ratio (P_{M+1}/P_M) in the Biofield Energy Treated 6-mercaptopurine was significantly decreased by 42.49% compared with the control sample **(Table 1)**. Therefore, it was concluded that the ^{13}C, ^{2}H, ^{15}N, and ^{33}S contributions from $(C_5H_5N_4S)^+$ to *m/z* 154 in the Biofield Energy Treated sample were significantly decreased compared to the control sample.

Table 1. LC-MS based isotopic abundance analysis results of 6-mercaptopurine in Biofield Energy Treated sample compared to the control sample.

Parameter	Control sample	Biofield Energy Treated sample
P_M at *m/z* 153 (%)	100	100
P_{M+1} at *m/z* 154 (%)	8.19	4.71
P_{M+1}/P_M	0.08	0.05
% Change of isotopic abundance ratio (P_{M+1}/P_M) with respect to the control sample		-42.49

P_M: The relative peak intensity of the parent molecular ion [M^+]; P_{M+1}: the relative peak intensity of the isotopic molecular ion [(M+1) $^+$], M: mass of the parent molecule

Gas chromatography-mass spectrometry (GC-MS) analysis

The GC-MS of the control and Biofield Energy Treated 6-mercaptopurine showed the presence of the single chromatographic peak at the retention time of 16.04 min in the chromatogram **(Figures 4 and 5)**. The parent molecular ion peak of 6-mercaptopurine at *m/z* 152 $[M]^+$ (calculated for $C_5H_5N_4S^+$, 152.02) in the control sample and Biofield Energy Treated sample, along with the fragment ion peaks near *m/z* 119 and 70 **(Figures 4 and 5)** which were proposed corresponded to the molecular formula $C_5H_3N_4^+$ and $C_3H_6N_2^+$, respectively **(Figure 3)**. The mass peak intensities influence the isotopic abundance ratio, which was well supported by the LC-MS based isotopic abundance ratio analysis.

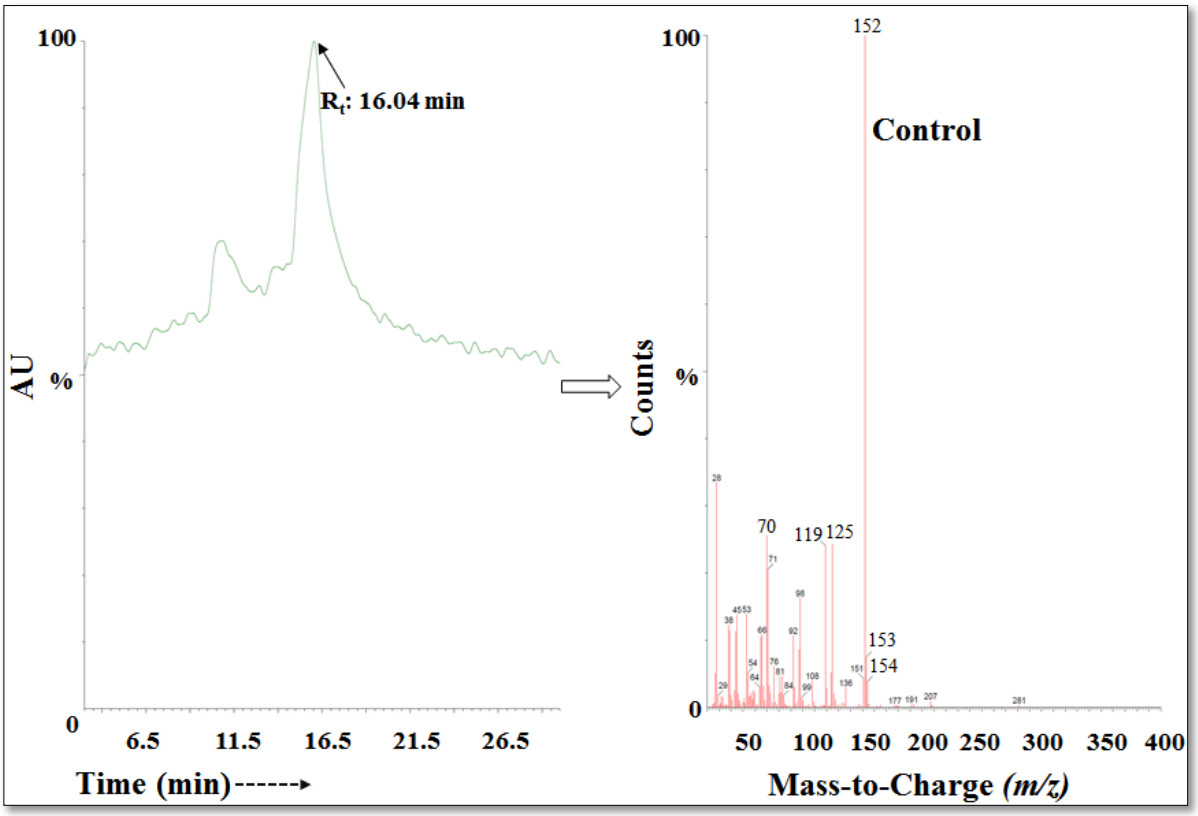

Figure 4. The GC-MS chromatogram and mass spectra of the control 6-mercaptopurine.

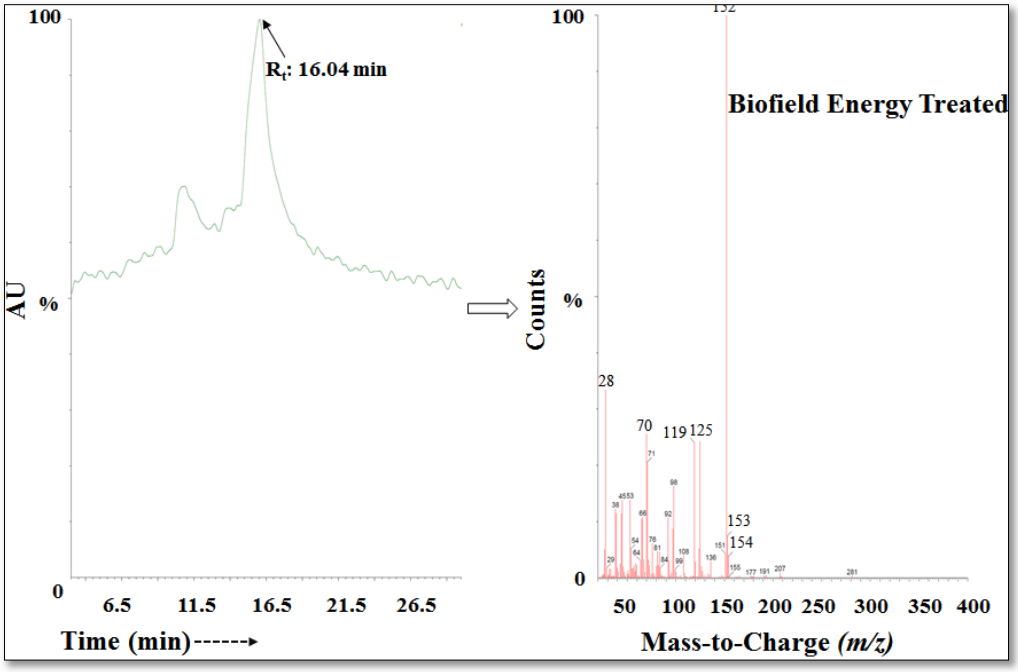

Figure 5. The GC-MS chromatogram and mass spectra of the Biofield Energy Treated 6-mercaptopurine.

The GC-MS spectra of both the control and Biofield Energy Treated 6-mercaptopurine showed the mass of the molecular ion peak $[M]^+$ at *m/z* 152 (calculated for $C_5H_4N_4S^+$, 152.02). The theoretical calculation of P_{M+1} for 6-mercaptopurine was presented as below:

P (^{13}C) = [(5 x 1.1%) x 100% (the actual size of the M^+ peak)] / 100% = 5.5%

P (^{2}H) = [(4 x 0.015%) x 100%] / 100%= 0.06%

P (^{15}N) = [(4 x 0.4%) x 100%] / 100% = 1.6%

P (^{33}S) = [(1 x 0.08%) x 100%] / 100% = 0.08%

$P_{M+1,}$ i.e., ^{13}C, ^{2}H, ^{15}N, and ^{33}S contributions from $(C_5H_5N_4S)^+$ to *m/z* 153 = 7.24%

From the above calculation, it has been found that ^{13}C and ^{15}N have a major contribution to *m/z* 153.

Similarly, the theoretical calculation of P_{M+2} for 6-mercaptopurine was presented as below:

P (^{34}S) = [(1 x 4.21%) x 100%] / 100% = 4.21%

$P_{M+2,}$ i.e., ^{34}S contributions from $(C_5H_5N_4S)^+$ to *m/z* 154 = 4.21%

From the above calculation, it has been found that only ^{34}S has a major contribution to *m/z* 153. The calculated isotopic abundances (4.21) were close to the experimental value of 3.8 **(Table 2)**.

The GC-MS based isotopic abundance ratio analysis of 6-mercaptopurine in the control and treated samples were calculated. $P_{M,}$ P_{M+1}, and P_{M+2} for 6-mercaptopurine near *m/z* 152, 153, and 154, respectively of the control and treated samples, which were obtained from the observed relative peak intensities of $[M^+]$, $[(M+1)^+]$, and $[(M+2)^+]$ peaks, respectively in the mass spectra and are presented in **Table 2**. The isotopic abundance ratio of P_{M+1}/P_M in the Biofield Energy Treated 6-mercaptopurine was decreased by 1.34% compared with the control sample **(Table 2)**. Hence, ^{13}C, ^{2}H, ^{15}N, and ^{33}S contributions from $(C_5H_5N_4S)^+$ to *m/z* 153 in the treated sample were decreased compared with the control sample. However, the isotopic abundance ratio of P_{M+2}/P_M in the treated was significantly increased by 11.58% compared with the control sample **(Table 2)**. Hence, ^{34}S contributions from $(C_5H_5N_4S)^+$ to *m/z* 154 in the treated sample were significantly increased compared with the control sample.

LC-MS and GC-MS study confirmed the structure of the sample as 6-mercaptopurine. The isotopic abundance ratios of P_{M+1}/P_M (^{2}H/^{1}H or ^{13}C/^{12}C or ^{15}N/^{14}N or ^{33}S/^{32}S) and P_{M+2}/P_M (^{34}S/^{32}S) in the treated sample were significantly altered compared to the control sample. As per modern physics, neutrinos change identities which are only possible if the neutrinos possess mass and could interchange their phase from one phase to another internally. Therefore, the neutrinos could interact with protons and neutrons in the nucleus, which indicated a close relation between neutrino and the isotope formation [19,40,41]. The altered isotopic composition at the molecular level of The Trivedi Effect®-Consciousness Energy Healing Treated 6-mercaptopurine might be due to the alteration in neutron to proton ratio in the nucleus. It can be hypothesized that the changes in isotopic abundance

could be due to changes in nuclei possibly through the interference of neutrino particles *via* The Trivedi Effect® - Consciousness Energy Healing Treatment. The new form of 6-mercaptopurine (Biofield Energy Treated) would be particularly useful to design better pharmaceutical formulations that might offer a better therapeutic response against many diseases.

Table 2. GC-MS based isotopic abundance analysis results of 6-mercaptopurine in control and Biofield Energy Treated samples.

Parameter	Control sample	Biofield Energy Treated sample
P_M at *m/z* 152 (%)	100.00	100.00
P_{M+1} at *m/z* 153 (%)	7.48	7.38
P_{M+1}/P_M	0.07	0.07
% Change of isotopic abundance ratio (P_{M+1}/P_M) with respect to the control sample		-1.34
P_{M+1} at *m/z* 154 (%)	3.80	4.24
P_{M+1}/P_M	0.04	0.04
% Change of isotopic abundance ratio (P_{M+2}/P_M) with respect to the control sample		11.58

P_M: The relative peak intensity of the parent molecular ion [M^+]; P_{M+1}: the relative peak intensity of the isotopic molecular ion [$(M+1)^+$]; P_{M+2}: the relative peak intensity of the isotopic molecular ion [$(M+2)^+$], M: Mass of the parent molecule

CONCLUSIONS

The experimental results concluded that The Trivedi Effect®-Consciousness Energy Healing Treatment showed a significant impact on the isotopic abundance ratios and mass peak intensities of 6-mercaptopurine. The LC-MS based isotopic abundance ratio of P_{M+1}/P_M ($^2H/^1H$ or $^{13}C/^{12}C$ or $^{15}N/^{14}N$ or $^{33}S/^{32}S$) in the Biofield Energy Treated 6-mercaptopurine was significantly decreased compared with the control sample. Thus, ^{13}C, ^2H, ^{15}N, and ^{33}S contributions from $(C_5H_5N_4S)^+$ in the Biofield Energy Treated sample were significantly decreased compared with the control sample. The GC-MS based isotopic abundance ratio of P_{M+1}/P_M in the Biofield Energy Treated 6-mercaptopurine was decreased as compared with the control sample. Hence, ^{13}C, ^2H, ^{15}N, and ^{33}S contributions from $(C_5H_5N_4S)^+$ in the Biofield Energy Treated sample were significantly decreased compared with the control sample. However, the isotopic abundance ratio of P_{M+2}/P_M in the Biofield Energy Treated 6-mercaptopurine was significantly increased compared with the control sample. Hence, ^{18}O contributions from $(C_5H_5N_4S)^+$ in the Biofield Energy Treated sample were significantly increased compared with the control sample. It can be assumed that the changes in isotopic abundance and mass peak intensities could be due to changes in nuclei possibly through the interference of neutrino particles via The Trivedi Effect® - Consciousness Energy Healing Treatment (Biofield Energy Healing Treatment). The new form of Biofield Energy Treated 6-mercaptopurine would be better designing novel pharmaceutical formulations that might offer a better therapeutic response against acute lymphocytic leukemia, chronic myeloid leukemia, Crohn's disease, and ulcerative colitis, etc.

ACKNOWLEDGMENTS

The authors are grateful to the Sophisticated Instrumentation Centre for Applied Research & Testing (SICART) India, Trivedi Science, Trivedi Global, Inc., Trivedi Testimonials, and Trivedi Master Wellness for their assistance and support during this work.

REFERNCES

1. Salser JS, Balis ME (1965) The Mechanism of Action of 6-Mercaptopurine: I. Biochemical Effects. Cancer Res 25: 539-543.
2. Dubinsky MC (2004) Azathioprine, 6-mercaptopurine in inflammatory bowel disease: Pharmacology, efficacy and safety. Clin Gastroenterol Hepatol 2(9): 731-743.
3. Present DH, Korelitz BI, Wisch N, Glass JL, Sachar DB, et al. (1980) Treatment of Crohn's disease with 6-mercaptopurine: A long-term, randomized, double-blind study. N Engl J Med 302: 981-987.
4. Schmiegelow K, Glomstein A, Kristinsson J, Björk O, Salmi T, et al. (1997) Impact of morning versus evening schedule for oral methotrexate and 6-mercaptopurine on relapse risk for children with acute

lymphoblastic leukemia. Nordic Society for Pediatric Hematology and Oncology (NOPHO). J Pediatr Hematol Oncol 19: 102-109.

5. Sack DM, Peppercorn MA (1983) Drug therapy of inflammatory bowel disease. Pharmacotherapy 3: 158-176.
6. World Health Organization (2015) 19th WHO Model List of Essential Medicines (April 2015). Available online at: https://www.who.int/medicines/publications/essentialmedicines/EML2015_8-May-15.pdf
7. Mercaptopurine (2020) Available online at: https://en.wikipedia.org/wiki/Mercaptopurine
8. Yang JJ, Landier W, Yang W, Liu C, Hageman L, et al. (2015) Inherited NUDT15 variant is a genetic determinant of mercaptopurine intolerance in children with acute lymphoblastic leukemia. J Clin Oncol 33: 1235-1242.
9. Moriyama T, Nishii R, Perez-Andreu V, Yang W, Klussmann FA, et al. (2016) NUDT15 polymorphisms alter thiopurine metabolism and hematopoietic toxicity. Nature Genet 48: 367-373.
10. Lerner EI, Flashner-Barak M, Achthoven EV, Keegstra H, Smit R (2012) Formulations of 6-mercaptopurine. US patent US8188067 B2.
11. Ade TB, Hjalgrim LL, Nersting J, Breitkreutz J, Nelken B, et al. (2016) Evaluation of a pediatric liquid formulation to improve 6-mercaptopurine therapy in children. Eur J Pharm Sci 83: 1-7.
12. National Center for Biotechnology Information (2020). PubChem Compound Summary for CID 667490, Mercaptopurine. Available online at: https://pubchem.ncbi.nlm.nih.gov/compound/Mercaptopurine
13. Chereson R (2009) Basic pharmacokinetics. 1st ed. Pharmaceutical Press, London.
14. Trivedi MK, Patil S, Shettigar H, Bairwa K, Jana S (2015) Spectroscopic characterization of biofield treated 6-mercaptopurine and tinidazole. Med Chem 5: 340-344.
15. Trivedi MK, Mohan R, Branton A, Trivedi D, Nayak G, et al. (2015) Evaluation of biofield energy treatment on physical and thermal characteristics of selenium powder. J Food Nutr Sci 3: 223-228.
16. Branton A, Jana S (2017) The influence of energy of consciousness healing treatment on low bioavailable resveratrol in male *Sprague Dawley* rats. Int J Clin Dev Anatomy 3: 9-15.
17. Trivedi MK, Branton A, Trivedi D, Nayak G, Panda P, et al. (2016) Evaluation of the isotopic abundance ratio in biofield energy treated resorcinol using gas chromatography-mass spectrometry technique. Pharm Anal Acta 7: 481.
18. Trivedi MK, Branton A, Trivedi D, Nayak G, Sethi KK, et al. (2016) Determination of isotopic abundance ratio of biofield energy treated 1,4-dichlorobenzene using gas chromatography-mass spectrometry (GC-MS). Mod Chem 4: 30-37.
19. Trivedi MK, Mohan TRR (2016) Biofield energy signals, energy transmission and neutrinos. Am J Mod Phys 5: 172-176.
20. Rubik B (2002) The biofield hypothesis: Its biophysical basis and role in medicine. J Altern Complement Med 8: 703-717.
21. Nemeth L (2008) Energy and biofield therapies in practice. Beginnings 28: 4-5.
22. Rivera-Ruiz M, Cajavilca C, Varon J (2008) Einthoven's string galvanometer: The first electrocardiograph. Tex Heart Inst J 35: 174-178.
23. Rubik B, Muehsam D, Hammerschlag R, Jain S (2015) Biofield science and healing: History, terminology and concepts. Glob Adv Health Med 4: 8-14.
24. Koithan M (2009) Introducing complementary and alternative therapies. J Nurse Pract 5: 18-20.
25. Barnes PM, Bloom B, Nahin RL (2008) Complementary and alternative medicine use among adults and children: United States, 2007. Natl Health Stat Report 12: 1-23.
26. Trivedi MK, Tallapragada RM (2008) A transcendental to changing metal powder characteristics. Met Powder Rep 63: 22-28.
27. Trivedi MK, Nayak G, Patil S, Tallapragada RM, Latiyal O (2015) Studies of the atomic and crystalline characteristics of ceramic oxide nano powders after bio field treatment. Ind Eng Manage 4: 161.
28. Trivedi MK, Nayak G, Patil S, Tallapragada RM, Latiyal O, et al. (2015) Effect of biofield energy treatment on physical and structural properties of calcium carbide and praseodymium oxide. Int J Mater Sci Appl 4: 390-395.
29. Trivedi MK, Branton A, Trivedi D, Nayak G, Mondal SC, et al. (2015) Morphological characterization, quality, yield and DNA fingerprinting of biofield energy treated alphonso mango (*Mangifera indica* L.). J Food Nutr Sci 3: 245-250.
30. Trivedi MK, Branton A, Trivedi D, Nayak G, Mondal SC, et al. (2015) Evaluation of biochemical marker-

Glutathione and DNA fingerprinting of biofield energy treated *Oryza sativa*. Am J Bio Sci 3: 243-248.

31. Trivedi MK, Branton A, Trivedi D, Nayak G, Charan S, et al. (2015) Phenotyping and 16S rDNA analysis after biofield treatment on *Citrobacter braakii*: A urinary pathogen. J Clin Med Genom 3: 129.
32. Trivedi MK, Patil S, Shettigar H, Mondal SC, Jana S (2015) Evaluation of biofield modality on viral load of Hepatitis B and C viruses. J Antivir Antiretrovir 7: 083-088.
33. Trivedi MK, Patil S, Shettigar H, Bairwa K, Jana S (2015) Phenotypic and biotypic characterization of *Klebsiella oxytoca*: An impact of biofield treatment. J Microb Biochem Technol 7: 203-206.
34. Nayak G, Altekar N (2015) Effect of biofield treatment on plant growth and adaptation. J Environ Health Sci 1: 1-9.
35. Ansari SA, Trivedi MK, Branton A, Trivedi D, Nayak G, et al. (2018) *In vitro* effects of biofield energy treated vitamin D_3 supplementation on bone formation by osteoblasts cells. Biomed Sci 4: 10-17.
36. Koster DA, Trivedi MK, Branton A, Trivedi D, Nayak G, et al. (2018) Evaluation of biofield energy treated vitamin D_3 on bone health parameters in human bone osteosarcoma cells (MG-63). Biochem Mol Biol 3: 6-14.
37. Trivedi MK, Patil S, Shettigar H, Mondal SC, Jana S (2015) The potential impact of biofield treatment on human brain tumor cells: A time-lapse video microscopy. J Integr Oncol 4: 141.
38. Trivedi MK, Patil S, Shettigar H, Gangwar M, Jana S (2015) *In vitro* evaluation of biofield treatment on cancer biomarkers involved in endometrial and prostate cancer cell lines. J Cancer Sci Ther 7: 253-257.
39. Schellekens RC, Stellaard F, Woerdenbag HJ, Frijlink HW, Kosterink JG (2011) Applications of stable isotopes in clinical pharmacology. Br J Clin Pharmacol 72: 879-897.
40. Weisel CP, Park S, Pyo H, Mohan K, Witz G (2003) Use of stable isotopically labeled benzene to evaluate environmental exposures. J Expo Anal Environ Epidemiol 13: 393-402.
41. Muccio Z, Jackson GP (2009) Isotope ratio mass spectrometry. Analyst 134: 213-222.
42. Rosman KJR, Taylor PDP (1998) Isotopic compositions of the elements 1997 (Technical Report). Pure Appl Chem 70: 217-235.
43. Smith RM (2004) Understanding Mass Spectra: A Basic Approach. Second Edition, John Wiley & Sons, Inc.
44. Jürgen H (2004) Gross Mass Spectrometry: A Textbook 2nd edition. Springer: Berlin.